CHEMISTRY
A European Journal

A Journal of
ChemPubSoc Europe

Accepted Article

Title: Acid-regulated Switching of Metal Cation and Anion Guest Binding in Halogen Bonding Rotaxanes

Authors: Xiaoxiong Li, Jason Y.C. Lim, and Paul D. Beer

To be cited as: *Chem. Eur. J.* 10.1002/chem.201803902

Link to VoR: http://dx.doi.org/10.1002/chem.201803902

Supported by
ACES

WILEY-VCH

10.1002/chem.201803902

WILEY-VCH

Acid-regulated Switching of Metal Cation and Anion Guest Binding in Halogen Bonding Rotaxanes

Xiaoxiong Li,[a] Jason Y.C. Lim,[a] and Paul D. Beer*[a]

Abstract: The ability of natural enzymes to regulate their guest binding affinities and preferences through the use of co-ligands which alter the features of the binding site is fundamental to biological homeostatic control. Herein, the rarely-exploited orthosteric control of guest binding is demonstrated using neutral halogen bonding [2]rotaxanes, where a chemical stimulus (acid) interacting with the interlocked host binding site switches the host's native guest preference from metal cations to anions. When neutral, the rotaxanes exhibit pronounced transition metal cation affinity and comparatively weak anion binding properties. However, the addition of acid attenuates the rotaxanes' ability to coordinate cations, while concurrently enabling strong binding of halides through charge assisted halogen bonding and hydrogen bonding interactions in competitive aqueous solvent media. The appendage of a fluorescent anthracene reporter group to the rotaxane framework also enables diagnostic sensory responses to cation/ anion binding.

Introduction

In nature, enzymatic host-guest interactions governing biological processes are subject to natural regulatory feedback mechanisms which maintain enzymatic activity within stringent limits. This occurs primarily by changing the affinity of the enzyme to its target guest species, which can be achieved by either allosteric or orthosteric regulation,[1,2] and hence are both attractive targets for drug development.[3,4] Allosteric regulation, the process by which ligand binding at a site *distinct* from the guest binding cavity modulates the latter's guest affinity by changing its size and shape, has been demonstrated in numerous artificial biomimetic systems in recent years,[5–7] enabling applications such as controlled guest release in changing chemical media [8,9] and switchable catalysis.[10–12] The alternative orthosteric regulation mechanism, where direct ligand coordination within the original binding site itself changes its native guest affinity and selectivity, by comparison, has received scant attention in the design of abiotic host systems. Partly due to the significant challenges in designing receptors containing binding cavities capable of such chemical stimuli-responsive behaviour, existing systems capable of orthosteric regulatory binding are limited to pH-induced modulation of anion selectivity of acyclic pyridyl thioureas[13] and quaternary ammonium guest orientation within a cavitand host binding pocket.[14]

While we recently reported a rotaxane containing separate Lewis basic and acidic sites for simultaneously binding an axle separated sodium cation - halide anion ion-pair,[15] a mechanically bonded interlocked host system with the capability of switching from binding one class of guest species (e.g. cations) to another fundamentally-different class (e.g. anions) triggered simply by the orthosteric action of an external chemical stimulus (e.g. acid) is to the best of our knowledge unprecedented.

Herein, we report in this proof-of-concept study the first neutral halogen bonding (XB) [2]rotaxane hosts capable of orthosteric-regulated switching between cation and anion guest binding behaviour triggered by the presence of acid. XB is the attractive non-covalent interaction between electron-deficient halogen atoms and Lewis bases such as anions, which has been shown to outperform analogous hydrogen bonding (HB) receptors in competitive solvent media.[16,17]

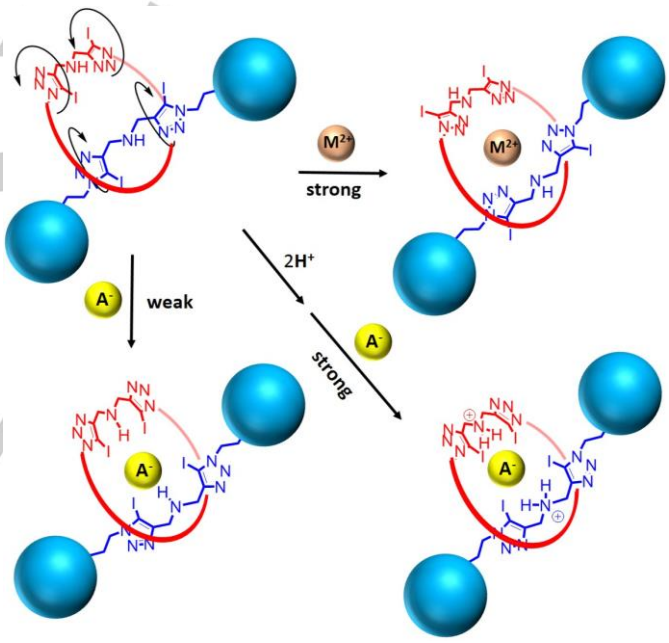

Figure 1. Schematic illustration showing dual capability of rotaxane to bind anions and metal cations *via* exo-endo dentate conformational inversion of iodotriazole motifs.

In our rotaxane design (Figure 1), we integrate a novel XB bis-iodotriazole-secondary amine functional motif into the axle and macrocycle components of the mechanically interlocked molecule (MIM) structural framework. The conformational flexibility of the combined antagonistic Lewis basic (triazole and secondary amine N-donors) and Lewis acidic XB (iodotriazole) groups facilitates the rotaxane in the neutral state to bind transition metal cations *via* bis-tridentate N-donor coordination and to bind anions relatively weakly through XB and HB interactions. Protonation of the secondary amine functionalities, concomitant with the conformational inversion of the XB iodotriazole motifs, activates the binding cavity for strong charge assisted XB and HB anion coordination in competitive aqueous

[a] X. Li, Dr J.Y.C Lim, Prof. P.D. Beer
Chemistry Research Laboratory, Department of Chemistry
University of Oxford, 12 Mansfield Road, Oxford, OX1 3TA (UK)
E-mail: paul.beer@chem.ox.ac.uk

Supporting information (SI) for this article is given via a link at the end of the document.

solvent media whilst concurrently attenuating metal cation binding. Notably, the mechanically-interlocked nature of the rotaxanes is integral to this orthosteric acid-regulation of binding preferences, which maintains the highly-preorganised nature of the cavity to facilitate guest binding, whilst also allowing sufficient *endo*/*exo* flexibility of the iodotriazole motifs for anion/cation coordination within the rotaxane cavity. We also demonstrate that the appendage of an anthracene reporter group to the rotaxane host expedites the diagnostic fluorescence sensing of both metal cation and anion binding in neutral and protonated states.

Results and Discussion

Synthesis of Rotaxanes

The target neutral [2]rotaxanes were constructed using the active metal template (AMT) strategy,[18,19] where coordination of a metal catalyst within the cavity of a macrocycle facilitates the formation of a covalent bond between appropriately-functionalised axle precursors. Despite the presence of the electron-withdrawing iodine atoms of iodotriazole motifs, we have previously shown that the triazole nitrogen atoms are sufficiently basic for coordination to Cu(I),[20] allowing

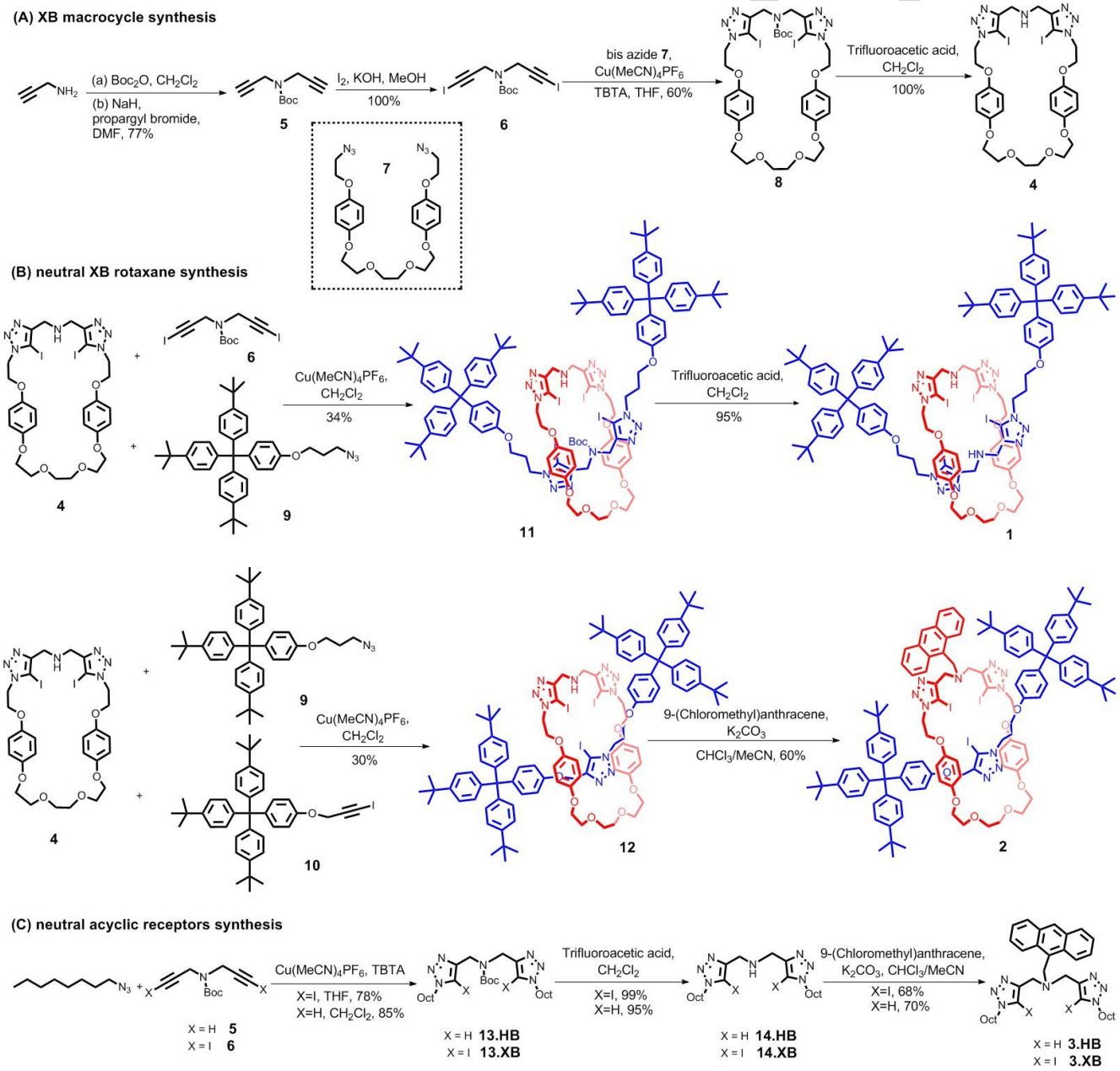

Scheme 1. Synthesis of (A) secondary amine-containing XB macrocycle **4** and (B) Neutral XB rotaxanes **1** and **2** (C) Neutral acyclic receptors **3.XB** and **3.HB**.

the AMT approach to be used for the synthesis of a series of [2]rotaxanes containing XB interlocked cavities for halide binding[20–22] and chiral oxoanion discrimination[23] with the copper(I)-catalysed azide-(iodo)alkyne cycloaddition (CuAAC) reaction. In the novel rotaxane design described herein (Figure 1), the presence of the central Lewis basic amine motif of the macrocycle component is expected to facilitate Cu(I) coordination for CuAAC-AMT rotaxane assembly.[24,25]

The synthesis of the key XB macrocycle component **4** is summarised in Scheme 1A. *N*-Boc-protected bis-alkyne **5** was prepared in two steps from reaction of Boc-anhydride with propargyl amine[26] followed by addition of sodium hydride and propargyl bromide. The reaction of iodine with **5** under basic conditions afforded the bis-iodinated-alkyne intermediate **6** in quantitative yield. CuAAC macrocycle ring-closing of equimolar amounts of **6** with bis-azide **7**[27] under high-dilution conditions afforded *N*-Boc-protected macrocycle **8** in 60 % yield. The high yield of the XB macrocycle synthesis reaction is especially noteworthy, given the lack of a template used to facilitate macrocyclisation over non-productive formation of acyclic oligomers. Subsequent *N*-Boc-deprotection with trifluoroacetic acid (TFA) afforded the target XB macrocycle **4** quantitatively.

With macrocycle **4** (1.0 equiv.), CuAAC-AMT rotaxane formation was performed using a stoichiometric quantity of $[Cu(CH_3CN)_4]PF_6$ in dichloromethane with either bis-iodoalkyne **6** (4.0 equiv.) and stoppered azide **9** (8.0 equiv.); or azide **9** (5.0 equiv.) and stoppered-iodoalkyne **10** (5.0 equiv.) (Scheme 1B). This method afforded neutral rotaxanes **11** and **12** in 34 % and 30 % isolated yields respectively after Cu(I) decomplexation and chromatographic purification. The interlocked nature of both rotaxanes **11** and 1**2** was evident from the diagnostic upfield shifts of their macrocycle components' hydroquinone protons resulting from aromatic donor-acceptor π-π stacking interactions with the axle units' iodotriazole motifs (Figures S2-10 and S2-16, SI), and conclusively demonstrated with ^{1}H-^{1}H ROESY spectroscopy (Figures S2-45 and S2-46, SI). Target neutral XB rotaxane **1** was then produced by *N*-Boc-deprotection of the axle component of rotaxane **11** using trifluoroacetic acid (TFA). The fluorescent anthracene-appended rotaxane **2** was prepared *via* the reaction of rotaxane **12** with 9-(chloromethyl)anthracene under basic conditions. Anthracene-appended acyclic receptors **3.XB** and **3.HB** were also synthesised through similar protocol (see Section S1, SI, for full synthetic details).

Guest Binding Properties of Neutral Rotaxanes

Rotaxanes **1** and **2** contain multiple iodotriazole motifs flanking their three-dimensional interlocked cavities, which are capable of multi-dentate anion binding interactions *via* their Lewis acidic XB-donor iodine atoms.[20] The presence of methylene spacers immediately adjacent to the iodotriazole units provides sufficient flexibility for endo/exo-dentate flipping of the iodotriazoles such that their Lewis basic nitrogen atoms[28] can also coordinate to metal cations within the rotaxanes' cavities, aided by the proximal secondary amine donor units.

The anion binding properties of both rotaxanes were first probed by ^{1}H NMR titration experiments, where increasing quantities of anions, as their tetrabutylammonium (TBA) salts, were added to separate solutions of rotaxanes **1** and **2** in d_6-acetone. As shown in Figure 2A, the addition of Cl^- to rotaxane **1** resulted in downfield shifts of H_2 and H_d as well as significant upfield shifts of H_c, H_1, and H_4. Notably, the perturbations of these signals, arising from protons flanking the interlocked binding cavity containing the iodotriazole units, suggest that Cl^- was binding in its vicinity. At the same time, anion binding resulted in conformational changes to the rotaxane framework, evident from the shifts of the macrocycle component's hydroquinone proton signals and those from the axle's proximal stopper protons H_b. Similarly, the ^{1}H NMR spectrum of rotaxane **2** displayed considerable changes upon Cl^- addition (Figure 2B),

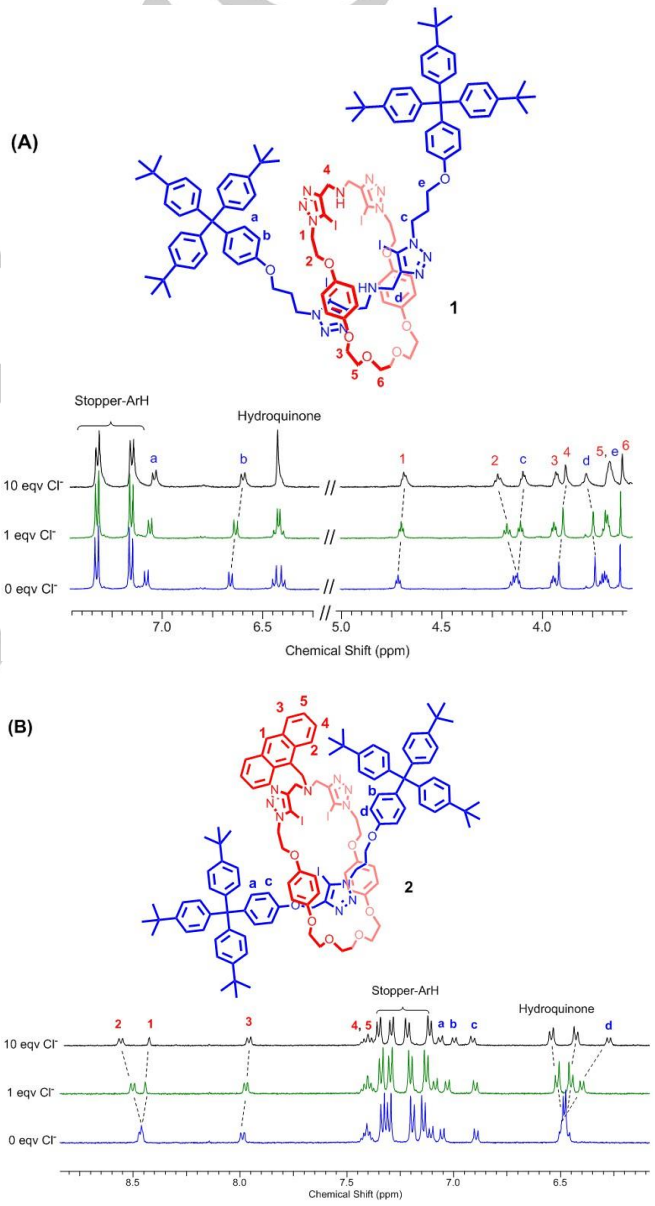

Figure 2. Partial ^{1}H NMR spectra of neutral rotaxanes (A) **1** and (B) **2** in the presence of 0.0, 1.0 and 10.0 equivalents of Cl^- in d_6-acetone ([rotaxane] = 1.0 mM, *T* = 298 K).

most notably the downfield shift of H_2 on the macrocycle's anthracene unit and a large upfield shift of axle proton H_d, suggesting that the halide was binding just above the interlocked cavity. WinEQNMR2[29] analysis of the ^{1}H NMR titration data, monitoring the shifts of protons H_b and H_2 of rotaxanes **1** and **2** respectively as a function of anion concentration, afforded host-guest 1:1 stoichiometric association constants (K_a/M^{-1}) summarised in Table 1.

Table 1. Association constants (*K*a [M^{-1}]) of halides with neutral rotaxanes **1** and **2**, as well as acyclic receptors **3.XB** and **3.HB** in d_6-acetone. [a]

	Rotaxane **1**	Rotaxane **2**	Receptor **3.XB**	Receptor **3.HB**
Cl^-	(8.0 ± 0.1) x 10^2	(8.2 ± 0.1) x 10^2	(7.2 ± 0.3) x 10^1	(1.5 ± 0.1) x 10^1
Br^-	-c	(3.4 ± 0.1)x 10^2	-b	-b

[a] Values of K_a are calculated by the WinEQNMR2[29] software using a 1:1 host-guest stoichiometric binding model. Errors (±) are in parentheses (<10%). No binding observed for NO_3^- to rotaxane **1**. No binding observed for I^-, NO_3^- and ReO_4^- to rotaxane **2**.

[b] no binding. [c] not conducted.

From Table 1, both rotaxanes **1** and **2** show comparable affinities for Cl^- in d_6-acetone despite the former's greater number of XB-donor iodotriazole units. This may be a consequence of rotaxane **2**'s more preorganised cavity due to a lower number of conformationally-flexible methylene units, and the bulky anthracene unit favouring endo-orientation of the XB donor iodine atoms on the macrocycle component for convergent anion coordination. Compared with Cl^-, rotaxane **2** binds Br^- more weakly, which is likely to be a consequence of its lower charge density. Interestingly, no significant interactions of rotaxane **2** with I^-, $NO_3^-$and ReO_4^- were observed, presumably due primarily to their poor shape/size-complementarity with the rotaxane's binding cavity. Similarly, rotaxane **1** did not show any binding to NO_3^-. Nonetheless, both rotaxanes were found to bind Cl^- with K_a values more than an order-of-magnitude larger than acyclic model receptor **3.XB** (Table 1), which emphasizes the importance of the preorganised rotaxane interlocked cavity and convergent XB interactions for anion coordination. Furthermore, the greatly-enhanced Cl^- affinity of **3.XB** compared to its acyclic HB receptor analogue **3.HB** highlights the superiority of XB over HB for anion binding. When the ^{1}H NMR titration experiments of rotaxanes **1** and **2** with Cl^- were repeated in the more competitive solvent mixture of $CDCl_3/CD_3OD$ (1:1 v/v), no evidence of anion binding was found.

The appendage of the anthracene reporter group to rotaxane **2**'s macrocycle component also enabled the host to sense anions *via* fluorescence responses. In acetonitrile, rotaxane **2** exhibits fluorescence emission between 370 and 530 nm which is typical of an anthracene emission spectrum[30] (Figure 3). In the presence of Cl^-, significant fluorescence enhancement was observed, likely due to rigidification of the rotaxane framework upon anion binding which reduces the likelihood of non-radiative decay pathways.[31–33] Similar enhancement of fluorescence intensity was observed for acyclic receptors **3.XB** and **3.HB** upon Cl^- addition in acetonitrile (Figures S4-1 and S4-2, SI).

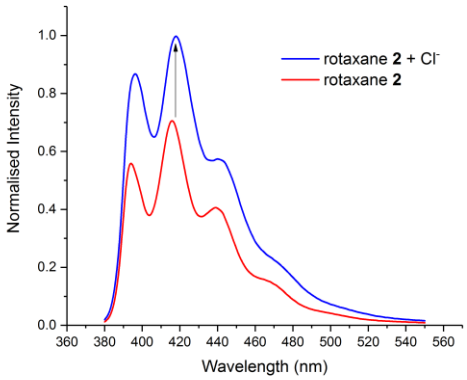

Figure 3. Fluorescence spectra of rotaxane **2** in the presence of 200 equivalents of Cl^- ([rotaxane **2**] = 5 μM, *T* = 293 K, solvent = CH_3CN, λ_{ex} = 368 nm).

Having probed the anion binding, and with rotaxane **2,** the fluorescence anion sensing properties of the MIMs, we investigated the possibility of using the rotaxanes as multidentate ligands for the coordination of metal cations. The complexation reaction of **1** with Zn^{2+} was performed under ambient conditions by stirring a solution of the neutral rotaxane with equimolar $Zn(ClO_4)_2{\cdot}6H_2O$ in CH_2Cl_2/ CH_3OH 1:1 *v/v* to afford the Zn^{2+}-bound rotaxane in quantitative yield. A comparison of the ^{1}H NMR spectra of free rotaxane **1** and its Zn^{2+} complex revealed clear evidence of metal cation coordination (Figure 4A), with signals from protons H_2, H_4, H_c and H_d displaying large downfield shifts, while those of the polyether portion of the macrocycle component (H_3, H_5, H_6) exhibited very small perturbations. These observations indicated that Zn^{2+} was coordinating in the rotaxane cavity flanked by the two tridentate triazole-secondary amine N-donors of the MIM's axle and macrocycle components, and not interacting with the polyether group of the macrocycle. At the same time, increased splitting of the macrocycle component's hydroquinone signals was seen, showing that Zn^{2+} coordination further amplified the differences between both hydroquinone proton environments as a result of its interlocked cavity binding location. To confirm the participation of the iodotriazole N-donors in Zn^{2+} coordination, a qualitative UV-Vis titration was performed where 1.0 equivalent of $Zn(ClO_4)_2{\cdot}6H_2O$ was added to an acetonitrile solution of rotaxane **1**, resulting in an intensity decrease of the 290 nm absorbance peak (Figure S2-25, SI). These changes are consistent with those observed during triazole *N*-coordination to transition metal cations such as Cu^+[20,34] and Zn^{2+}[35] due to perturbations of the energy levels of the heterocycle's frontier molecular orbitals. It is noteworthy that the presence of methanol in the CH_2Cl_2/CH_3OH 1:1 *v/v* solvent mixture used to prepare the zinc (II) complex with **1,** was found to negate the rotaxane's ability to bind anions (*vide supra*). This observation clearly demonstrates that the neutral interlocked host **1** favours metal

cation binding over anions.[36] Unequivocal evidence of Zn^{2+} coordination within the rotaxane structure was obtained from high-resolution electrospray ionisation mass spectrometry (Figures S2-24, SI).

With rotaxane **2**, the binding of different transition metal cations, added as their perchlorate salts, in acetonitrile elicited contrasting fluorescence responses. The binding of closed-shell Zn^{2+} resulted in a dramatic increase in the rotaxane's fluorescence intensity (Figure 4B), which was likely primarily due to metal coordination of the Lewis basic lone pair on the macrocycle component's tertiary amine functionality responsible for photoinduced electron transfer (PET) quenching of the anthracene's fluorescence.[32,37] In stark contrast, the binding of redox-active Cu^{2+} and Ni^{2+} to rotaxane **2** elicited significant fluorescence quenching (Figure 4C and Figure S4-3, SI, respectively) which probably results from an electron transfer quenching mechanism from the photoexcited anthracene moiety to the respective transition metal centre.[38,39]

Acid-triggered Changes in Rotaxane Guest Binding Behaviour

After demonstrating the predisposition of the neutral binding cavities of both rotaxanes **1** and **2** for metal cation coordination over chloride anion recognition in methanol containing solvent media, the orthosteric modulation of their binding properties upon protonation was investigated. The effects of protonation on the structure of the neutral [2]rotaxanes was initially investigated using ^{1}H NMR spectroscopy. As shown in Figure 5A, upon the addition of 2.0 equivalents of HBF_4 to a solution of rotaxane **1** in $CDCl_3$/ CD_3OD/ D_2O (45:45:10 *v/v/v*), the largest downfield shift was observed for proton signal H_4 immediately adjacent to the secondary amine moiety on the macrocycle ($\Delta\delta$ = +0.4 ppm), consistent with increased electron-deficiency arising from protonation of the adjacent amine unit. At the same time, perturbations of the signals arising from the macrocycle component's polyether unit (H_3, H_5, H_6) may be attributed to HB interactions between the protonated ammonium moiety on the axle and the oxygen atoms. This is also likely to restrict the rotational freedom of the macrocycle unit around the axle, resulting in greater desymmetrisation of the macrocycle hydroquinone protons. Notable conformational changes of the rotaxane framework occur upon protonation as well, as evident from the dramatic upfield signal shift of axle proton H_d ($\Delta\delta$ = -0.2 ppm), possibly as a result of increased shielding from the macrocycle hydroquinone motifs. These structural changes, as well as being in close proximity to a dicationic bis-protonated rotaxane cavity, result in notable deshielding and downfield shifts of axle proton signals H_b, H_c and H_e. Compared to rotaxane **1**, the changes upon addition of one equivalent of HBF_4 to rotaxane **2**'s ^{1}H NMR spectrum are more modest, owing to its single tertiary amine moiety available for protonation (**Figure S3-9**, SI). Notably however, the largest downfield shift was also observed for the anthracene methylene protons H_6 adjacent to the ammonium unit ($\Delta\delta$ = +0.4 ppm), with the

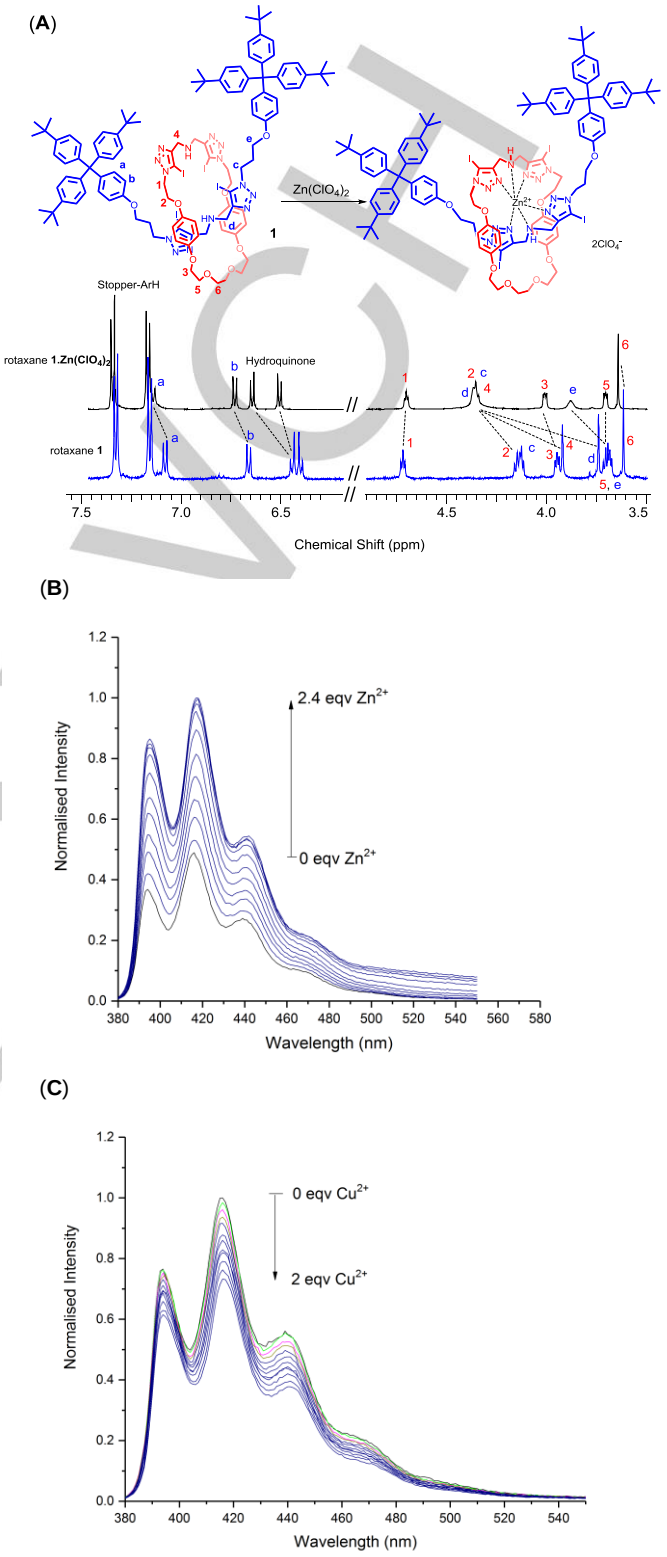

Figure 4. (A) ^{1}H NMR spectra of free rotaxane **1** and its Zn^{2+} complex in d_6-acetone showing the effects of cation association ([rotaxane **1**] = 2 mM, *T* = 298 K); Fluorescence spectra of rotaxane **2** before and after addition of (B) Zn^{2+} and (C) Cu^{2+}. (λ_{ex} = 368 nm, solvent = CH_3CN)

axle protons next to the iodotriazole moiety showing much smaller shifts. This clearly indicates that despite the presence of Lewis basic nitrogen atoms on the iodotriazoles, the amine unit is preferentially protonated. In further support, HBF_4 addition to rotaxane **2** led to a large turn-on fluorescence response from the anthracene fluorophore (Figure S4-4, SI), which results from the loss of PET fluorescence quenching pathways upon amine protonation.[32,37,40,41]

The cationic binding cavities of rotaxanes [**1**•2H$^+$](BF$_4^-$)$_2$ and [**2**•H$^+$]BF$_4^-$ were now expected to bind anions strongly in competitive solvent media. Indeed, in the organic-aqueous solvent mixture $CDCl_3$/ CD_3OD/ D_2O (45:45:10 *v/v/v*), Cl^- addition to rotaxane [**1**•2H$^+$](BF$_4^-$)$_2$ once again elicited numerous changes to its ^{1}H NMR spectrum (Figure 5A), the most noteworthy of which are the downfield shifts of H_d and H_4, which likely arise from anion binding in close proximity to the interlocked cavity which results in further structural changes to the rotaxane. For rotaxane [**2**•H$^+$]BF$_4^-$ in $CDCl_3$/ CD_3OD (1:1 *v/v*), an upfield shift was observed for the corresponding macrocycle methylene protons H_{10} after addition of Cl^-, showing clear hydrogen bonding between Cl^- to the protonated tertiary ammonium unit (Figure S3-10, SI). These changes are especially notable given that the neutral rotaxanes **1** and **2** showed no evidence of interaction with anions in protic methanolic solvent media, further demonstrating the greatly augmented anion affinities of the protonated rotaxanes' cavities. While the direct involvement of HB from the cationic ammonium motifs in anion binding could not be unambiguously determined from ^{1}H NMR titrations, fluorescence titrations proved insightful. As shown in Figure 5B, addition of 80 equivalents of Cl^- to rotaxane [**2**•H$^+$]BF$_4^-$ in acetonitrile resulted in an approximately 60 % reduction in fluorescence intensity, attributable to strong ammonium - Cl^- HB interactions which partially restore the PET quenching properties of the macrocycle's amine moiety. In the more competitive solvent mixture of $CHCl_3$/ CH_3OH 1:1 *v/v*, a considerably smaller fluorescence 'turn-off' quenching response was recorded after adding the same amount of Cl^- anion (Figure 5B), consistent with greater competition from the protic solvent mixture for HB interactions with the highly charge-dense Cl^-. Nonetheless, by monitoring the ^{1}H NMR shifts of protons H_{10} of the protonated rotaxanes as a function of anion concentration, host-guest 1:1 stoichiometric association constants were determined using the WinEQNMR2[29] software, and compared with those of acyclic protonated receptors [**3XB**•H$^+$]BF$_4$ and [**3HB**•H$^+$]BF$_4$ (Table 2).

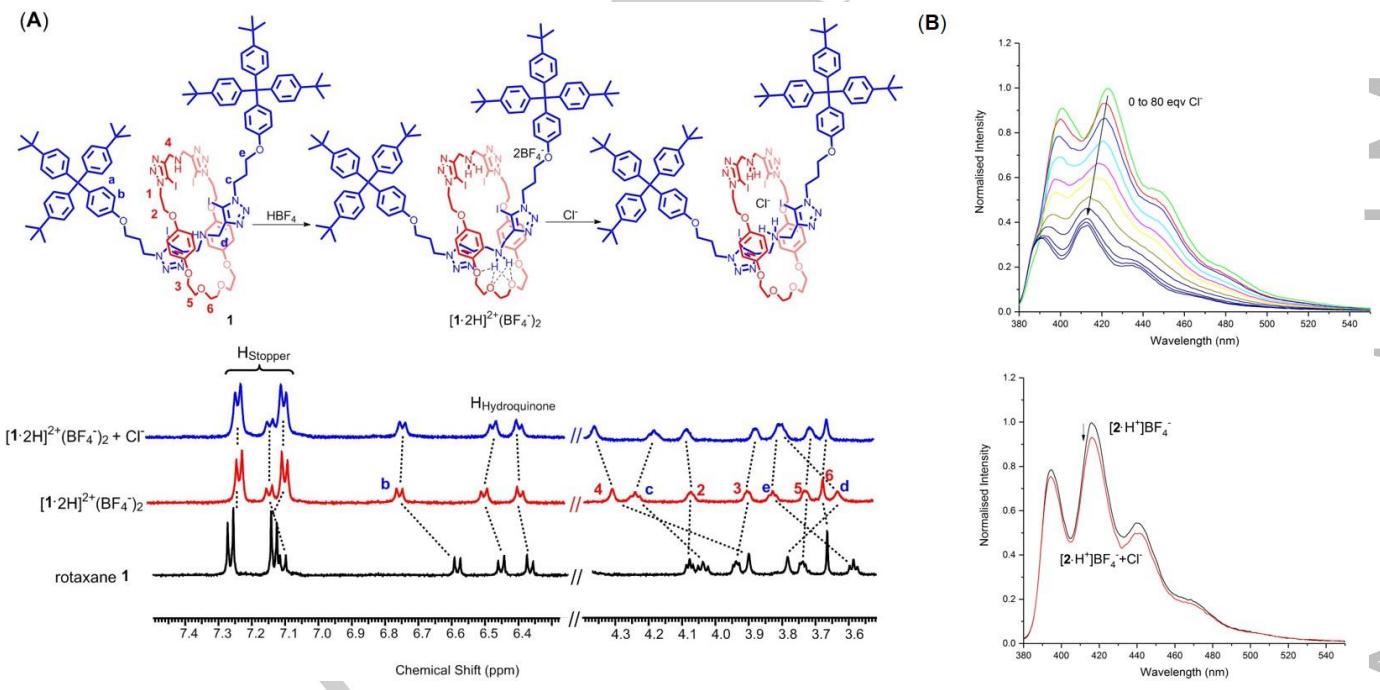

Figure 5. (A) Partial ^{1}H NMR spectra of neutral rotaxane **1** and doubly-protonated [**1**•2H$^+$](BF$_4^-$)$_2$ in the presence of 0 and 10 equivalents of TBACl ([host] = 1.0 mM, $CDCl_3$/ CD_3OD/ D_2O 45:45:10 *v/v/v*, *T* = 298 K); (B) Fluorescence spectra showing the changes in anthracene fluorescence intensity of singly-protonated rotaxane [**2**•H$^+$]BF$_4^-$ upon Cl^- addition in acetonitrile (top) and $CHCl_3$/ CH_3OH 1:1 *v/v* (bottom) ([host] = 5 μM , *T* = 298K, λ_{ex} = 368 nm)

Table 2. Association constants (K_a [M^{-1}]) of anions with cationic rotaxanes [**1**•2H$^+$](BF$_4^-$)$_2$ and [**2**•H$^+$]BF$_4^-$, as well as acyclic receptors [**3XB**•H$^+$]BF$_4^-$ and [**3HB** •H$^+$]BF$_4^-$. [a]

	[**1**•2H$^+$](BF$_4^-$)$_2$ [b]	[**2**•H$^+$]BF$_4^-$ [c]	[**3XB**•H$^+$]BF$_4^-$ [c]	[**3HB**•H$^+$]BF$_4^-$ [c]
Cl^-	(8.1 ± 0.1) x 10^2	(6.6 ± 0.1) x 10^2	(4.9 ± 0.4) x 10^2	(1.0 ± 0.1) x 10^2
Br^-	(4.8 ± 0.4) x 10^2	[d]	[e]	[e]
NO_3^-	(5.8 ± 0.4) x 10^2	[d]	[e]	[e]

[a] Values of K_a are calculated by the WinEQNMR2[29] software using a 1:1 host-guest stoichiometric binding model, monitoring proton H_8 and H_9 (**Figure S3-12** and **Figure S3-13**, **SI**) respectively. Errors (±) are in parentheses (<10%). No binding observed for I^- and ReO_4^- with both [**1**•2H$^+$](BF$_4^-$)$_2$ and [**2**•H$^+$]BF$_4^-$. [b] Performed in $CDCl_3$/ CD_3OD/ D_2O 45:45:10 *v/v* monitoring H_4. [c] Performed in $CDCl_3$/ CD_3OD 1:1 *v/v*. [d] no binding. [e] not conducted

As shown in Table 2, both protonated XB rotaxane hosts display notable affinities for Cl^- in the competitive protic solvent medium. Importantly, for [**1**•2H$^+$](BF$_4^-$)$_2$, an anti-Hofmeister binding trend was observed for the anions tested, with the less strongly-hydrated anions Br^- and NO_3^- more weakly bound than Cl^-. No appreciable binding was observed for I^- and ReO_4^-, which may be due to their inability to fit into the preorganised rotaxane cavity. Given the inherent preference of XB donor host molecules to bind to the heavier and 'softer' halides in aqueous solvents due to their greater ease of dehydration,[16,20,42,43] this result is especially notable since it is the first example of an XB rotaxane preferentially binding the most strongly-hydrated Cl^- in the presence of water, and only the second XB receptor known to display an anti-Hofmeister binding bias.[44] While rotaxane [**1**•2H$^+$](BF$_4^-$)$_2$ displays stronger Cl^- binding compared to [**2**•H$^+$]BF$_4^-$, which is likely to be a consequence of its dicationic character, [**2**•H$^+$]BF$_4^-$ displayed rare exclusive Cl^- selectivity. Once again, the importance of XB interactions for anion binding, even with the contribution of HB interactions from the ammonium group(s), can be seen from the significantly stronger Cl^- binding affinities of protonated XB acyclic receptor [**3XB**•H$^+$]BF$_4$ compared with [**3HB**•H$^+$]BF$_4$. Hence the observed Cl^- selectivity for both rotaxanes is likely to result from a combination of favourable ammonium HB- and XB-chloride interactions together with a preorganised interlocked binding cavity which is of complementary shape and size to the halide guest species.

In contrast to anion binding, as expected the addition of acid proved highly detrimental to the rotaxanes' inherent metal cation affinity. Upon addition of 2.0 equivalents of HBF_4 to a solution of Zn^{2+}-complexed rotaxane **1** in d_6-acetone, considerable broadening of its ^{1}H NMR spectrum was observed, accompanied by the appearance of multiple additional peaks (Figure S2-26, SI) which is indicative of Zn^{2+} displacement from the rotaxane's binding cavity, resulting from protonation of the amine units. Metal cation displacement from the binding cavity of rotaxane **2** upon protonation was also supported by fluorescence spectroscopy. For the Zn^{2+}, Cu^{2+} and Ni^{2+}-bound complexes of rotaxane **2**, the addition of 1.0 equivalent of HBF_4 resulted in significant fluorescence 'turn-on' responses suggesting the respective metal cation's displacement from the rotaxane cavity by protonation of the macrocycle component's tertiary amine unit (Figures S4-5 – S4-7, SI).

Conclusions

In conclusion, we have constructed the first examples of MIM hosts which, by virtue of their novel antagonistic Lewis basic triazole-secondary amine and Lewis acidic XB bis-iodotriazole functional motifs, are capable of acid-triggered switching of metal cation and anion guest binding behaviour. When neutral, the rotaxanes are capable of strong metal cation binding whereas anions are bound relatively weakly. Importantly, upon protonation the greatly augmented anion affinities observed for the cationic protonated rotaxanes also results in the unprecedented observation of anti-Hofmeister anion binding bias for Cl^- in aqueous solvent media by XB [2]rotaxanes. Furthermore, the presence of the anthracene fluorophore in rotaxane **2** allowed distinctive and diagnostic fluorescence responses towards the identity of guest species bound within its cavity. Overall, this present work demonstrates a rare example of orthosteric regulation of guest binding in abiotic receptors, which is unprecedented with MIM hosts, where the proton acts as the orthosteric ligand protonating the rotaxane interlocked binding cavity to significantly modulate guest binding preferences. This simple, yet effective method of switching between metal cation and anion binding in interlocked host structures heralds new possibilities in their applications as molecular sensors, organocatalysts and molecular machines.[45–47]

Acknowledgements

X.L. thanks the CSC (China Scholarship Council) for a postgraduate scholarship. J.Y.C.L. thanks the Agency for Science, Technology and Research (A*STAR), Singapore, for postdoctoral funding support.

Keywords: halogen bonding • rotaxane • orthosteric regulation • anion recognition • transition metal recognition

References

[1] W. M. Nolte, J.-P. Fortin, B. D. Stevens, G. E. Aspnes, D. A. Griffith, L. R. Hoth, R. B. Ruggeri, A. M. Mathiowetz, C. Limberakis, D. Hepworth, et al., *Nat. Chem. Biol.* **2014**, *10*, 629.

[2] Y. Zheng, L. Qin, N. V. O. Zacarías, H. de Vries, G. W. Han, M. Gustavsson, M. Dabros, C. Zhao, R. J. Cherney, P. Carter, et al., *Nature* **2016**, *540*, 458.

[3] T. S. Mohamed, S. S. Jayakar, A. K. Hamouda, *Front. Mol. Neurosci.* **2015**, *8*, DOI 10.3389/fnmol.2015.00071.

[4] R. Nussinov, C.-J. Tsai, *Curr. Pharm. Des.* **2012**, *18*, 1311–1316.
[5] W. J. Ramsay, J. R. Nitschke, *J. Am. Chem. Soc.* **2014**, *136*, 7038–7043.
[6] J. Mendez-Arroyo, J. Barroso-Flores, A. M. Lifschitz, A. A. Sarjeant, C. L. Stern, C. A. Mirkin, *J. Am. Chem. Soc.* **2014**, *136*, 10340–10348.
[7] J. Kuwabara, H. J. Yoon, C. A. Mirkin, A. G. DiPasquale, A. L. Rheingold, *Chem. Commun.* **2009**, *0*, 4557–4559.
[8] M. Yamanaka, M. Kawaharada, Y. Nito, H. Takaya, K. Kobayashi, *J. Am. Chem. Soc.* **2011**, *133*, 16650–16656.
[9] S. Javor, J. Rebek, *J. Am. Chem. Soc.* **2011**, *133*, 17473–17478.
[10] K. Eichstaedt, J. Jaramillo-Garcia, D. A. Leigh, V. Marcos, S. Pisano, T. A. Singleton, *J. Am. Chem. Soc.* **2017**, *139*, 9376–9381.
[11] V. Blanco, A. Carlone, K. D. Hänni, D. A. Leigh, B. Lewandowski, *Angew. Chem. Int. Ed.* **2012**, *51*, 5166–5169.
[12] V. Blanco, D. A. Leigh, U. Lewandowska, B. Lewandowski, V. Marcos, *J. Am. Chem. Soc.* **2014**, *136*, 15775–15780.
[13] S. Rashdan, M. E. Light, J. D. Kilburn, *Chem. Commun.* **2006**, *0*, 4578–4580.
[14] Y. J. Kim, M. T. Lek, M. P. Schramm, *Chem. Commun.* **2011**, *47*, 9636–9638.
[15] R. C. Knighton, P. D. Beer, *Chem. Commun.* **2014**, *50*, 1540–1542.
[16] A. Brown, P. D. Beer, *Chem. Commun.* **2016**, *52*, 8645–8658.
[17] L. C. Gilday, S. W. Robinson, T. A. Barendt, M. J. Langton, B. R. Mullaney, P. D. Beer, *Chem. Rev.* **2015**, *115*, 7118–7195.
[18] J. D. Crowley, S. M. Goldup, A.-L. Lee, D. A. Leigh, R. T. McBurney, *Chem. Soc. Rev.* **2009**, *38*, 1530.
[19] M. Denis, S. M. Goldup, *Nat. Rev. Chem.* **2017**, *1*, 0061.
[20] J. Y. C. Lim, T. Bunchuay, P. D. Beer, *Chem. – Eur. J.* **2017**, *23*, 4700–4707.
[21] M. J. Langton, Y. Xiong, P. D. Beer, *Chem. – Eur. J.* **2015**, *21*, 18910–18914.
[22] X. Li, J. Y. C. Lim, P. D. Beer, *Faraday Discuss.* **2017**, *203*, 245–255.
[23] J. Y. C. Lim, I. Marques, V. Félix, P. D. Beer, *J. Am. Chem. Soc.* **2017**, *139*, 12228–12239.
[24] T. R. Chan, R. Hilgraf, K. B. Sharpless, V. V. Fokin, *Org. Lett.* **2004**, *6*, 2853–2855.
[25] S. I. Presolski, V. Hong, S.-H. Cho, M. G. Finn, *J. Am. Chem. Soc.* **2010**, *132*, 14570–14576.
[26] P. Bonomi, M. D. Attieh, C. Gonzato, K. Haupt, *Chem. – Eur. J.* **2016**, *22*, 10150–10154.
[27] J. Y. C. Lim, I. Marques, A. L. Thompson, K. E. Christensen, V. Félix, P. D. Beer, *J. Am. Chem. Soc.* **2017**, *139*, 3122–3133.
[28] B. Schulze, U. S. Schubert, *Chem. Soc. Rev.* **2014**, *43*, 2522–2571.
[29] M. J. Hynes, *J. Chem. Soc. Dalton Trans.* **1993**, 311.
[30] B. Valeur, M. N. Berberan-Santos, *Molecular Fluorescence: Principles and Applications*, John Wiley & Sons, **2013**.
[31] A. Borissov, J. Y. C. Lim, A. Brown, K. E. Christensen, A. L. Thompson, M. D. Smith, P. D. Beer, *Chem. Commun.* **2017**, *53*, 2483–2486.
[32] R. Martínez-Máñez, F. Sancenón, *Chem. Rev.* **2003**, *103*, 4419–4476.
[33] P. D. Beer, *Acc. Chem. Res.* **1998**, *31*, 71–80.
[34] O. Fleischel, N. Wu, A. Petitjean, *Chem. Commun.* **2010**, *46*, 8454–8456.
[35] F. Otón, M. del C. González, A. Espinosa, A. Tárraga, P. Molina, *Organometallics* **2012**, *31*, 2085–2096.
[36] The paramagnetic nature of transition metal cations such as Cu^{2+} and Ni^{2+} precluded the use of ^{1}H NMR spectroscopy to study their binding to rotaxane **1**.
[37] R. R. Mittapalli, S. S. R. Namashivaya, A. S. Oshchepkov, E. Kuczyńska, E. A. Kataev, *Chem. Commun.* **2017**, *53*, 4822–4825.
[38] L. Fabbrizzi, A. Poggi, *Chem. Soc. Rev.* **1995**, *24*, 197–202.
[39] P. V. Bernhardt, B. M. Flanagan, M. J. Riley, *J. Chem. Soc. Dalton Trans.* **1999**, *0*, 3579–3584.
[40] D. H. Vance, A. W. Czarnik, *J. Am. Chem. Soc.* **1994**, *116*, 9397–9398.
[41] F. Sancenón, A. Benito, J. M. Lloris, R. Martínez-Máñez, T. Pardo, J. Soto, *Helv. Chim. Acta* **2002**, *85*, 1505–1516.
[42] M. J. Langton, L. C. Duckworth, P. D. Beer, *Chem. Commun.* **2013**, *49*, 8608–8610.
[43] M. J. Langton, P. D. Beer, *Chem. Commun.* **2014**, *50*, 8124–8127.
[44] D. Mungalpara, S. Stegmüller, S. Kubik, *Chem. Commun.* **2017**, *53*, 5095–5098.
[45] M. J. Chmielewski, J. J. Davis, P. D. Beer, *Org. Biomol. Chem.* **2009**, *7*, 415–424.
[46] R. Mitra, H. Zhu, S. Grimme, J. Niemeyer, *Angew. Chem. Int. Ed.* **2017**, *56*, 11456–11459.
[47] S. Erbas-Cakmak, D. A. Leigh, C. T. McTernan, A. L. Nussbaumer, *Chem. Rev.* **2015**, *115*, 10081–10206.

Entry for the Table of Contents (Please choose one layout)

Layout 1:

FULL PAPER

By virtue of their novel antagonistic Lewis basic triazole-secondary amine and Lewis acidic halogen bonding bis-iodotriazole functional motifs, mechanically bonded interlocked rotaxane hosts are capable of acid-triggered switching of metal cation and anion guest binding behaviour.

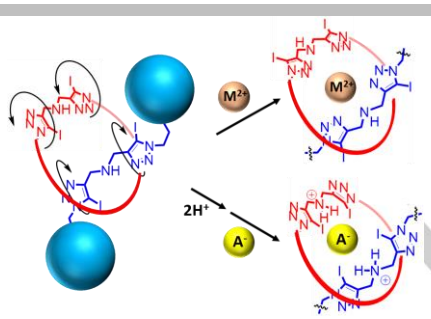

*X. Li, J.Y.C Lim, P.D. Beer**

Page No. – Page No.

Acid-regulated Switching of Metal Cation and Anion Guest Binding in Halogen Bonding Rotaxanes

Layout 2:

FULL PAPER

((Insert TOC Graphic here; max. width: 11.5 cm; max. height: 2.5 cm))

*Author(s), Corresponding Author(s)**

Page No. – Page No.

Title

Text for Table of Contents